Infrared photoluminescence of preexisting or irradiation-induced interstitial oxygen molecules in glassy SiO_2 and α-quartz

L. Skuja
PTB Braunschweig, Bundesallee 100, 38116 Braunschweig, Germany
and Institute of Solid State Physics, University of Latvia, Kengaraga 8, LV1063 Riga, Latvia

B. Güttler and D. Schiel
PTB Braunschweig, Bundesallee 100, 38116 Braunschweig, Germany

A. R. Silin
Institute of Solid State Physics, University of Latvia, Kengaraga 8, LV1063 Riga, Latvia
(Received 4 May 1998)

A sensitive technique for detecting interstitial O_2 molecules in SiO_2 is demonstrated by measuring their infrared $a \rightarrow X$ luminescence at 1272.2 nm under a Ti-sapphire laser excitation into the O_2 $X \rightarrow b$ absorption band at 765 nm. Contrary to the case of O_2 trapped in inert gas matrices, the visible emission of O_2 corresponding to the direct $b \rightarrow X$ transition is not found. Examination of different neutron- and gamma-irradiated glassy SiO_2 and α-quartz samples reveals radiation-induced interstitial oxygen molecules in concentrations between 10^{14} and 10^{16} molecules/cm^3. The radiolytic O_2 molecules in α-quartz and glassy SiO_2 experience different structural environments. [S0163-1829(98)00645-6]

I. INTRODUCTION

Silicon dioxide in its different forms (glass, amorphous oxide films, α-quartz) is presently the most extensively used wide-gap material in optics, microelectronics, and telecommunications. In most applications, point defects in SiO_2 play a detrimental role, a notable exception being the writing of fiber-optic Bragg gratings, which is facilitated by the presence of color centers. Despite the considerable research efforts in the past, a number of fundamental issues concerning the physics of defects and defect processes in SiO_2 are still insufficiently understood.

The basic intrinsic defects found in silica are: the ''E' center'' (paramagnetic positively charged oxygen vacancy $\equiv$Si$\cdot$Si$\equiv$ or neutral dangling Si bond, $\equiv Si\cdot$), the nonbridging oxygen hole center (''NBOHC,'' a dangling oxygen bond $\equiv$Si-O$\cdot$), the peroxy radical (''POR,'' $\equiv$Si-O-O$\cdot$) and the still controversial ''oxygen deficiency center'' (ODC), attributed either to a neutral oxygen vacancy $\equiv$Si-Si$\equiv$ or to a twofold-coordinated Si atom $\equiv$Si-O-Si-O-Si$\equiv$. The defects and defect processes in silica have been reviewed in Ref. 1.

The past studies have indicated that apart from the basic intrinsic defects in SiO_2 listed above, interstitial O_2 molecules take an important part in defect processes in SiO_2. They can be introduced into silica directly during the manufacturing process or by a subsequent high-temperature treatment of silica samples in O_2 atmosphere.[2] The main experimental proof of the presence of interstitial O_2 in SiO_2 has been the observed[3] growth of peroxy radical defect population at the expense of the E' centers in post-irradiation annealing experiments:

$$\equiv \mathrm{Si}\cdot + \mathrm{O_2} \rightarrow \equiv \mathrm{Si\text{-}O\text{-}O}\cdot. \qquad (1)$$

This reaction was suggested by Edwards and Fowler.[4] Their calculations demonstrated that the reaction is commensurate with the known O_2 diffusivity and E' center and POR concentrations, and they were subsequently experimentally verified.[2] On the basis of reaction (1) it was found that Suprasil W1 type silica is the most oxygen-saturated one among all available commercial types of silica, and that it contains around 10^{17} to 10^{18} molecules O_2/cm^3. The reaction (1) is reversible, and POR's can be destroyed by irradiation,[5] resulting in an E' center and an O_2 molecule.

While studies[2–5] have emphasized the role of O_2 in radiation processes in oxygen-saturated silicas, a more fundamental point is whether O_2 can be created *radiolytically* from the network oxygens in any SiO_2 glass, and what is the efficiency of the process. Tsai and Griscom[6] observed defect annealing behavior compatible with Eq. (1) after irradiating stoichiometric silica with pulses of an ArF excimer laser ($h\nu = 6.4$ eV). This serves as a proof that O atoms can be displaced from the glassy SiO_2 network in excitonic processes. Zhang *et al.*,[7] relying on Eq. (1), demonstrated recently that interstitial O_2 molecules are found even in oxygen deficient silicas under x-ray irradiation and concluded that they must be of radiolytic origin.

For closer investigations of oxygen displacement-related processes in SiO_2 a more straightforward spectroscopic method than the technique based on Eq. (1) would be useful. Two additional options for detecting interstitial O_2 have been demonstrated: by registering the $^1\Delta_g(\nu'=0) \rightarrow {}^3\Sigma_g^-(\nu''=0)$ near-infrared photoluminescence (PL) of O_2 at 1272.2 nm, excited with an Nd-YAG laser at 1064.1 nm,[8] and by measuring the visible-excited Raman line of the interstitial O_2 at 1549 cm^{-1} in optical fibers[9] and in bulk silica.[10] Both methods utilize highly specific spectral signatures of interstitial O_2, which permits unambiguous interpretation. The ad-

 ©1998 The American Physical Society

vantage of the Raman technique is that it allows absolute concentration measurements through comparison with the spectrum of gaseous O_2.[10] The sensitivity threshold of the method is $\approx 10^{17}$ molecules/cm^3. The main advantage of the Nd-laser excited infrared PL measurements is a higher sensitivity ($\approx 10^{16}$ molecules/cm^3). The disadvantage of the PL technique is the uncertainty whether the luminescence quantum yield and the oscillator strength of the excitation transition $X^3\Sigma_g^-(\nu''=0) \rightarrow a^1\Delta_g(\nu'=1)$ remain exactly constant in all SiO_2 matrices. The parameters of these forbidden transitions are very sensitive to the interactions between the interstitial molecule and the surrounding matrix: the radiative lifetime of the $a \rightarrow X$ transition is more than 1 h for an isolated O_2 molecule and decreases up to 10^4 times for O_2 dissolved in liquids.[11]

However, both methods are insufficiently sensitive to monitor the O_2 concentration in the 10^{14} to 10^{16} molecules/cm^3 range, i.e., in the region where the observation of ''intrinsic'' O_2 interstitials, created radiolytically from the bridging SiO_2 network oxygens has been reported.[7,12] Fortunately, the PL technique[8,12] leaves plenty ground for further improvements. The recent study of O_2 trapped in inert gas matrices[13] shows that the rate of the radiative transition from the second excited state of O_2 to the ground state, $b^1\Sigma_g^+ \rightarrow X^3\Sigma_g^-$, occurring in the 763 to 765 nm region, is 4 to 20 times larger than the rate of the $a^1\Delta_g \rightarrow X^3\Sigma_g^-$ transition, and that the conversion from the b to the a excited state is very efficient. This may point to the possibility of an effective excitation of the $a \rightarrow X$ transition of interstitial O_2 in silica via $X \rightarrow b$ excitation. An additional advantage is the large separation between the $X \rightarrow b$ excitation and $a \rightarrow X$ emission wavelengths, which allows the excitation energy to be tuned to the strongest feature in the $X \rightarrow b$ absorption spectrum (0-0 transition), as contrasted to the previous PL work[8] which relied on the approximate resonance of the Nd-YAG excitation laser wavelength with the weak vibrational sideband (0-1 transition) of the $X \rightarrow a$ zero-phonon line.

In the case of $X \rightarrow b$ excitation of O_2 in inert gas matrices, apart from the $a \rightarrow X$ emission, a weak $b \rightarrow X$ luminescence, Stokes-shifted against the excitation spectrum by 50 to 100 cm^{-1}, was also reported.[13]

The purposes of the present work were (i) to find out the efficiency and technical feasibility of exciting the $a \rightarrow X$ photoluminescence of O_2 in SiO_2 via the $X \rightarrow b$ absorption transition, (ii) to search for the direct $b \rightarrow X$ luminescence, (iii) to explore the low T region, and (iv) to apply this techniques to a set of differently irradiated SiO_2 samples to evaluate the radiolytic production of interstitial O_2.

II. EXPERIMENT

The samples of synthetic glassy and crystalline SiO_2 used in this work are described in Table I. Sample 1 of type Suprasil W1 is oxygen-rich, ''dry'' (contains less than 5×10^{-6} parts OH groups) and has been used in our previous Raman study.[10] Samples 2–5 of type Suprasil 3 and sample 6 of type Suprasil 2 are ''wet'' (contain $\approx 1 \times 10^{-3}$ parts OH groups) and are believed to be free from O_2 interstitials. Samples 7–11 of type KUVI are ''dry'' and oxygen deficient, as indicated by the relatively intense (0.4 cm^{-1}) optical absorption band at 245 nm in pristine samples which is due to oxygen deficiency-related intrinsic defects. The samples in groups 7–9 and 10–11 were cut from neighboring locations of the two respective glass blocks and, except for the effects of different irradiation histories, should have the same properties. The samples 12–15 are monocrystals of synthetic and natural (sample 15) α-quartz.

The fluencies of neutron irradiation indicated in Table I correspond to neutrons with energies above 1 keV. Samples 13 and 15 were irradiated in different facilities, therefore an accurate comparison of the doses received by them and by the other neutron-irradiated samples were not possible. The γ-ray exposure doses were measured relative to silicon.

The infrared luminescence spectra were measured with Bruker IFS-66 Fourier-transform spectrometer equipped with a FRA-106 Raman module and a liquid nitrogen-cooled Ge photodiode. The samples were excited either at $\lambda = 1064.1$ nm with a Nd-YAG laser (300 mW) in a backscattering geometry, or in the 690–770 nm region in right-angle geometry using a tunable Ti-sapphire laser (Spectra Physics 3900 S) pumped by an Ar^+-ion laser (Spectra Physics 2065-7S). The spectral resolution was 2 cm^{-1} and 4 cm^{-1}, respectively. The power of the Ti-sapphire laser was between 0.1 and 1 W, and it was verified that the luminescence signal remained linear with the excitation intensity.

The visible-range excitation spectrum of the infrared luminescence was measured manually point-by-point by tuning the Ti-sapphire laser, recording the luminescence spectrum and normalizing the integral intensity of the luminescence peak against the excitation laser photon flux at this wavelength.

The emission in the 765 nm region was measured under Ti-sapphire laser excitation with a triple Raman spectrometer (Instruments S.A. T64000) and a liquid N_2-cooled CCD camera in right-angle geometry.

For the low temperature measurements, the samples were placed in helium cryostats, suitable either for backscattering or right-angle geometries. Visible-excited infrared luminescence was measured only at room temperature.

III. RESULTS

Figure 1 shows the temperature effects on the Nd-YAG laser-excited infrared emission of interstitial O_2 in Suprasil W1 silica (sample 1). The room temperature spectrum is identical to that previously reported.[8] The relative wave number region from 0 to 1300 cm^{-1} is dominated by the Raman spectrum of fused silica, the peak in the 1535 cm^{-1} region is due to the O_2 luminescence. The absolute wave number and halfwidth of this peak are 7856 cm^{-1} and 86 cm^{-1}, respectively, at $T = 293$ K. On cooling to 10 K, the peak intensity grows ≈ 3 times, the halfwidth decreases to 26 cm^{-1}, and the maximum shifts to 7865 cm^{-1}.

When the excitation is shifted to 765 nm, a single intense luminescence peak at 7858.5 cm^{-1} (1272.2 nm) is observed (Fig. 2). With higher magnification, three Stokes-shifted sidebands 805, 1208, and 1548.5 cm^{-1} apart from the main peak are observed. A rough order-of-magnitude estimate of the decay time of this luminescence was attempted. The spectrometer data acquisition was started immediately after the exciting laser beam had been cut off, resulting in an ≈ 1 s effective delay between the excitation and the start of the

TABLE I. Fused silica and α-quartz samples used in this study and the calculated concentrations of interstitial O_2 molecules.

Sample no.	Sample type	Sample characterization	Irradiation	Intensity of O_2 emission, arb. units	Concentration of O_2, molecules/cm^3	Notes
1	glass	Suprasil W1 (type IV, dry)	none	81	8.0×10^{17}	[a]
2	glass	Type III, wet	gamma, 1.3 Grad	0.045	4.4×10^{14}	
3	glass	Type III, wet	2.2×10^{18} n/cm^2	0.702	6.9×10^{15}	
4	glass	Type III, wet	Gamma, 1.3 Grad	0.488	4.8×10^{15}	
5	glass	Type III, wet	2.2×10^{18} n/cm^2	0.146	1.4×10^{15}	
6	glass	Suprasil 2 (type III, wet)	none	not detected (<0.005)	not detected ($<5\times10^{13}$)	
7	glass	KUVI (dry, oxygen deficient)	2.2×10^{18} n/cm^2	0.088	8.7×10^{14}	
8	glass	KUVI (dry, oxygen deficient)	none	not detected (<0.005)	not detected ($<5\times10^{13}$)	[b]
9	glass	KUVI (dry, oxygen deficient)	2.2×10^{18} n/cm^2	0.132	1.3×10^{15}	
10	glass	KUVI (dry, oxygen deficient)	gamma, 1.3 Grad	0.021	2.1×10^{14}	
11	glass	KUVI (dry, oxygen deficient)	none	not detected (<0.005)	not detected ($<5\times10^{13}$)	[c]
12	α-quartz	synthetic	2.2×10^{18} n/cm^2	0.81	8.0×10^{15}	[d]
13	α-quartz	synthetic	10^{19} n/cm^2	2.193	2.2×10^{16}	[d]
14	α-quartz	synthetic	gamma, 1.3 Grad	not detected (<0.005)	not detected ($<5\times10^{13}$)	[d]
15	α-quartz	natural	10^{18} n/cm^2	0.0415	4.1×10^{14}	[d]

[a]Concentration calculated from the magnitude of the O_2 Raman line at 1549 cm^{-1} (Ref. 10).
[b]Control sample to sample 7.
[c]Control sample to samples 9 and 10.
[d]The concentration was estimated ignoring the possibly different luminescence efficiency of O_2 in quartz as compared to vitreous silica (see Sec. IV E).

measurement. The measurement duration was $\approx$5 s, corresponding to just a few interferometer scans. A very weak PL peak, similar to that depicted in Fig. 2, was recorded. This outcome indicates that this luminescence, or at least some component of it, has a decay time longer than $\approx$100 ms (assuming an exponential decay law).

The excitation spectrum of the 7858 cm^{-1} emission peak (Fig. 3) consists of two overlapping peaks. The main maximum occurs at 764.9 nm (13070 cm^{-1}). The attempts to fit the spectrum either with two Gaussians or two Lorentzians were only partially successful. The only consistent outcome of the fitting session was that both subbands of Fig. 3 are located 50 to 65 cm^{-1} apart.

The 7858 cm^{-1} emission can be excited in the 690 nm region as well (Fig. 4). A complete excitation spectrum in the vicinity of this wavelength was not measured. The luminescence intensity, normalized to the laser photon flux, was 14 times weaker under the 690.9 nm excitation, as compared with the case of 765 nm excitation.

Figure 5 shows the emission from Suprasil W1 silica in the 765 nm region under a near-resonance excitation in the maximum of the ''765 nm'' excitation band of Fig. 3, recorded at $T=10$ K. The spectrum obtained is similar to the conventional room-temperature Raman spectrum of silica, measured with 514.5 nm Ar line excitation (Fig. 5). Similar Raman scattering-dominated emission spectra (not shown) were recorded for 762 and 760 nm excitation as well.

The effects of irradiation on the 1272 nm emission peak

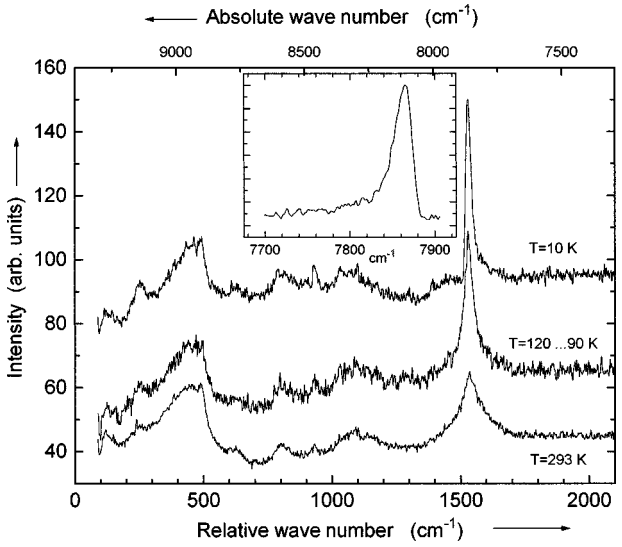

FIG. 1. Luminescence/Stokes Raman spectrum of Suprasil W1 fused silica under Nd-YAG laser ($\lambda = 1064.1$ nm) excitation, measured at $T = 293$ K (bottom), 120 K (middle), and at 10 K (top). The spectra were measured under identical laser power and detector gain, they are shifted vertically for visibility. The inset shows in absolute wave numbers the region of the O_2 emission line at 7865 cm^{-1} ($T = 10$ K). The absolute wave number of the luminescence peak at $T = 293$ K is 7856 cm^{-1}. The resolution is 2 cm^{-1}.

intensity are shown in Fig. 6. In both the ''wet'' [Fig. 6(a)] and the oxygen-deficient ''dry'' silicas [Fig. 6(b)] there is no measurable PL intensity in unirradiated samples. On the other hand, the 1272 nm luminescence band is found in every γ- or neutron-irradiated glass sample. The intensities of the radiation-induced PL bands are lower than 1% of the intensity in unirradiated Suprasil W1 silica. The luminescence was generally stronger in neutron-irradiated samples as compared with the γ-irradiated ones.

In the case of neutron-irradiated α-quartz monocrystals,

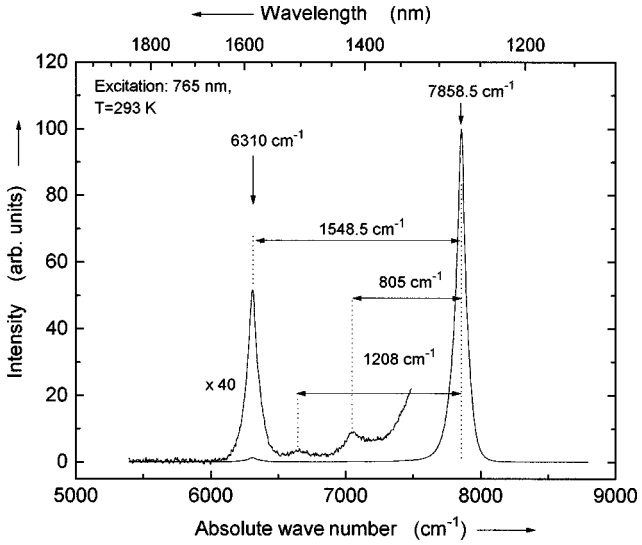

FIG. 2. Photoluminescence spectrum of Suprasil W1 fused silica recorded at $T = 293$ K under photoexcitation at 765 nm (titanium-sapphire laser).

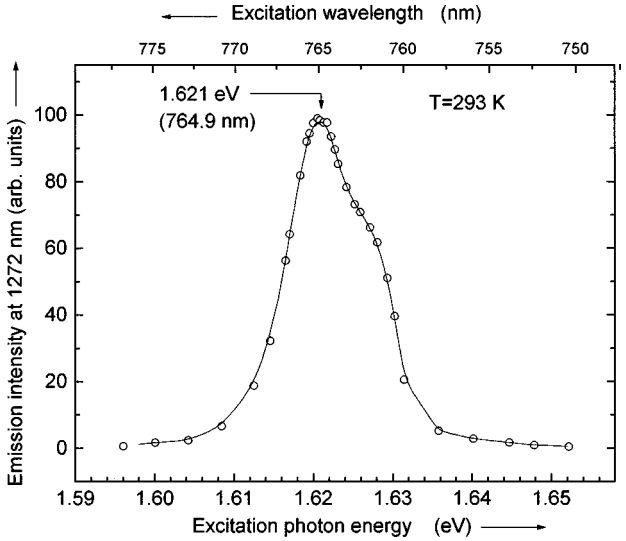

FIG. 3. Excitation spectrum of the $a^1\Delta_g \rightarrow X^3\Sigma_g^-$ photoluminescence transition at 1272 nm of interstitial oxygen molecules in Suprasil W1 fused silica, measured in the region of $O_2\, X^3\Sigma_g^-(\nu'' = 0) \rightarrow b^1\Sigma_g^+(\nu' = 0)$ transition. Circles: measured data points; the solid line is a guide to eye.

very similar PL bands are observed (Fig. 7). The PL intensity is the strongest in crystal 13, exposed to the largest irradiation dose (10^{19} neutrons/cm^2). The peak position occurs at 7805 cm^{-1}, it is shifted by $\approx$50 cm^{-1} to lower energies, relative to the PL peak position in vitreous silica.

In the less irradiated (2.2×10^{18} neutrons/cm^2) quartz crystal (sample 12) the PL peak may consist of two subbands: while its left wing is similar to that of the sample 13, the right wing is shifted by 6–8 cm^{-1} to higher energies and the peak region appears flattened. The PL peak in this region is observable as well in the crystal 15, irradiated by 10^{18} neutrons/cm^2, however, the intensity is too low to per-

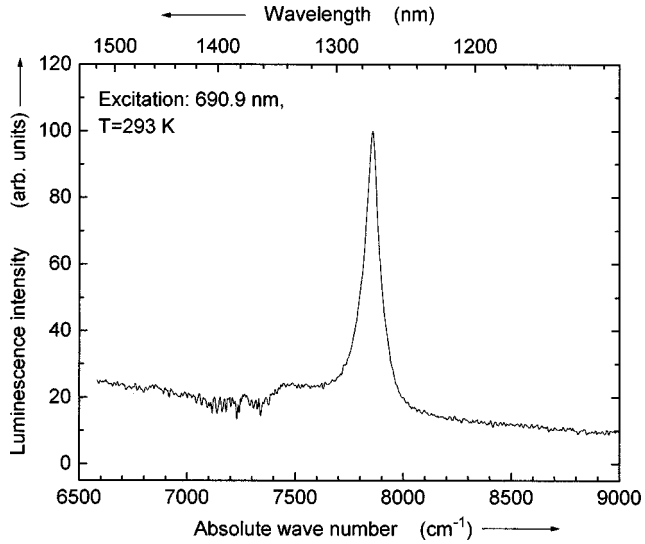

FIG. 4. Photoluminescence spectrum of Suprasil W1 fused silica recorded at $T = 293$ K under photoexcitation at $\lambda = 690.9$ nm in the region of the first vibronic sideband of the oxygen molecule $X \rightarrow b$ absorption $[^3\Sigma_g^-(\nu'' = 0) \rightarrow {}^1\Sigma_g^+(\nu' = 1)$ transition].

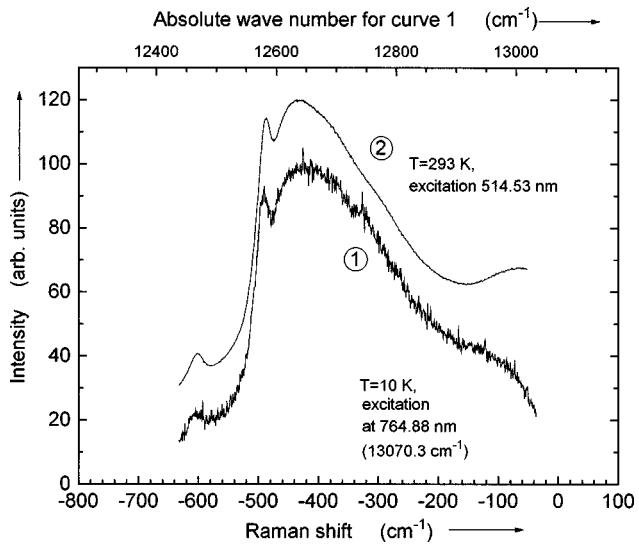

FIG. 5. Search for the $b \rightarrow X$ photoluminescence band of interstitial O_2 in Suprasil W1 fused silica. The spectrum (1) is recorded under Ti-sapphire laser excitation at 764.88 nm at sample temperature $T = 10$ K and resolution 4 cm^{-1}. The excitation wavelength corresponds to the maximum of the excitation spectrum for the $a \rightarrow X$ emission band of interstitial O_2 in silica (see Fig. 2). The absolute wave numbers are indicated at the top x-axis. The spectrum (2) is the conventional Raman spectrum of the same sample, recorded at $T = 293$ K under Ar laser 514.53 nm line excitation (bottom x axis valid only). The baseline of the spectrum (2) is shifted up by 20 arb. units.

mit a meaningful comparison with the band shapes of more strongly irradiated samples 13 and 12.

No trace of the PL band around 7800 cm^{-1} was found in the 1.3 Grad γ-irradiated quartz crystal (sample 14).

IV. DISCUSSION

A. Temperature effects on the Nd-YAG laser-excited luminescence of O_2

One of the main objectives of this work was to search for a high-sensitivity technique to detect the interstitial O_2 molecules in SiO_2. The detection thresholds of the Raman[10] measurements and Nd-YAG laser-excited room-temperature infrared O_2 $a \rightarrow X$ luminescence[8] are about 10^{17} and 10^{16} molecules/cm^3, respectively. The quantum yield Q of the $a \rightarrow X$ luminescence in SiO_2 is presently not known. In the case of O_2 molecules in solution (benzene) the Q has been measured as 5×10^{-5} at room temperature,[14] while in the case of O_2 trapped in Xe matrix $Q \approx 1$ at $T = 6$ K.[13] It could be expected that, for O_2 in SiO_2, Q is significantly below unity at room temperature. The quantum yield depends on the rates of the radiative (k_r) and nonradiative transitions (k_{nr}) from the excited state:

$$Q = k_r/(k_r + k_{nr}), \tag{2}$$

where $(k_r + k_{nr})^{-1} = \tau$ is the experimentally observable luminescence decay constant. Lowering of temperature could yield a significant increase in luminescence intensity due to the freezing-out of thermally activated nonradiative processes ($k_{nr} \rightarrow 0$).

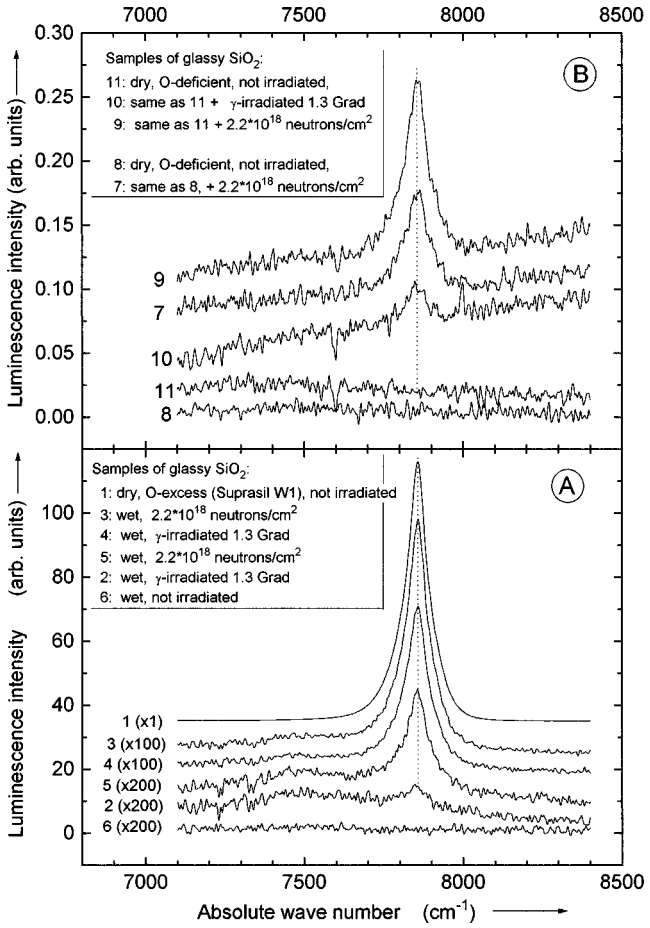

FIG. 6. Photoluminescence spectra of ''wet'' (a) and oxygen-deficient ''dry'' (b) synthetic fused silicas in the region of interstitial O_2 emission, measured at 765 nm excitation at $T = 293$ K. The curve numbers correspond to the sample numbering in Table I. The same y-scale is used in parts (a) and (b), curves are arbitrarily shifted vertically. The spectrum of the oxygen-rich ''dry'' Suprasil W1 silica (curve 1) is shown in part (a) for comparison.

However, the increase of the luminescence peak amplitude on cooling from 293 to 10 K is only moderate ($\approx$3 times, Fig. 1). Moreover, the increase is achieved mainly through the narrowing of the peak: the integral intensities at 120 or 10 K, calculated over the 1330–1705 cm^{-1} range are only $\approx$30% above the room temperature value. This finding could be indicative of relatively low k_{nr} values for the $a \rightarrow X$ transition of O_2 in SiO_2 ($k_{nr} \leqslant k_r$) and consequently, contrary to the initial expectations, of a quantum yield, higher by orders of magnitude at room temperature (probably between 0.1 and 1) than reported[14] for O_2 dissolved in benzene. Before such tentative conclusion is drawn, one must consider, however, that the $a \rightarrow X$ transition of an isolated O_2 molecule is highly forbidden and is enhanced in condensed matrices by low-symmetry interactions between O_2 and the surroundings. This may give rise to significant temperature dependence of the absorption cross section of the excitation transition and of the radiative transition rate k_r. If they decrease on cooling, the increase of the intensity due to the decreased rate of nonradiative transitions k_{nr} may be partially cancelled out.

Another evidence which may hint to a relatively high Q value for the $a \rightarrow X$ transition in SiO_2 is the rough observa-

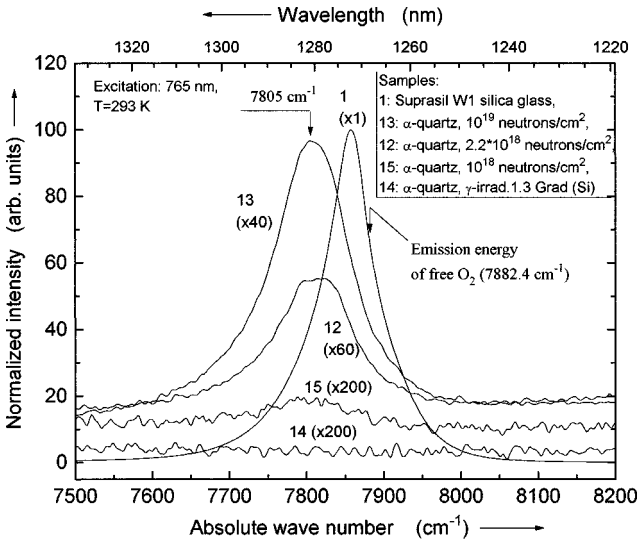

FIG. 7. Comparison of the photoluminescence emission spectra of interstitial O_2 molecules in fused silica (sample 1) and irradiated α-quartz (samples 12–15) measured under excitation at 765 nm. Sample numbers correspond to those in Table I. The respective gain factors are indicated at each curve.

tion of a long luminescence decay time $\tau \geqslant 100$ ms (see the Results section above). A low value of Q is commonly associated with a short observable τ [$\tau=(k_r+k_{nr})^{-1}=Q/k_r$]. For example, the $a\rightarrow X$ transition of O_2 in benzene with $Q=4.7\times10^{-5}$ has a τ value of 31 μs.[15] Assuming that k_r is of the same order of magnitude in both media, the quantum yield Q for O_2 in silica should be above 0.13. Further measurements of τ at different temperatures are necessary to determine the Q value with higher accuracy.

B. The nature of 765 nm and 690 nm excited luminescence in Suprasil W1 silica

The PL band at 7858.5 cm^{-1} observed at 765 nm excitation (Fig. 2) practically coincides with the PL band at 7856 cm^{-1} observed with 1064.1 nm excitation (Fig. 1 and Refs. 8, 10, and 12) and evidently has the same origin: the $a\ ^1\Delta_g(\nu'=0)\rightarrow X\ ^3\Sigma_g^-(\nu''=0)$ transition of interstitial O_2. The band at 6310 cm^{-1} (Fig. 2) is due to the transition terminating on the first vibrational level of the ground state, $^1\Delta_g(\nu'=0)\rightarrow{}^3\Sigma_g^-(\nu''=1)$. The splitting between the 6310 and 7858.5 cm bands, 1548.5 cm^{-1}, is equal to the ground state vibrational quantum of O_2 in silica, determined[9,10] from the Raman spectrum. A similar vibrational sideband, 1549 cm^{-1} from the main luminescence peak, was observed under Nd-YAG laser excitation.[8] The two low intensity peaks in the 6500 to 7000 cm^{-1} region are evidently due to phonon sidebands of the 7858 cm^{-1} PL peak, their energy shifts relative to the main PL peak correspond to the 800 and 1200 cm^{-1} longitudinal optical phonon modes[16] of silica.

The excitation spectrum of the 7858 cm^{-1} PL band with the peak at 764.9 nm (Fig. 3) clearly is due to the $X^3\Sigma_g^-(\nu''=0)\rightarrow b\ ^1\Sigma_g^+(\nu''=0)$ transition of interstitial O_2 in SiO_2. This zero-phonon transition occurs at 765 nm in liquid O_2 and between 763.9 and 764.8 nm in O_2 trapped in rare gas matrices.[13] A weak optical absorption band (ca. 0.5 to 3 db/km) corresponding to this transition has been reported in oxygen-saturated silica optical fibers.[17,9,18]

The expected approximate peak position of the $X^3\Sigma_g^-(\nu''=0)\rightarrow b\ ^1\Sigma_g^+(\nu''=1)$ excitation band can be estimated using the reported size of the vibrational quantum in the b excited state of an isolated O_2 molecule: 1404 cm^{-1}.[19] The vibration energy in the ground state is 6 cm^{-1} lower for O_2 in silica as compared with a free molecule. Assuming a similar vibrational frequency reduction in the b excited state, the expected peak position is $(13070+1398=14468)$ cm^{-1} or 690.9 nm. Indeed, an excitation at this wavelength yields $a\rightarrow X$ emission (Fig. 4). The excitation efficiency at 690.9 nm is equal to the efficiency of excitation at 758 nm, i.e., in the wing of the main excitation band, and it is much higher than at 750 nm (Fig. 3). This confirms that there exists an additional maximum in the excitation spectrum in the wavelength region below 750 nm. Its intensity is equal or above to 1/14 of the 765 nm excitation peak intensity. The exact peak position in the vicinity of $\lambda=691$ nm is yet to be measured.

The mechanism of the excitation of $a\rightarrow X$ luminescence via the $X\rightarrow b$ transition comprises an intermediate transition $b\rightarrow a$. The rate of this electric quadrupole transition in an isolated O_2 molecule is very low (1.7×10^{-3} s^{-1}); the corresponding emission band is known as the Noxon band with the 0-0 transition energy around 5240 cm^{-1} ($\lambda=1908$ nm).[19] The transition rate is significantly enchanced for O_2 in solutions. In the case of O_2 in CCl_4 the transition is observed at 1926 nm with a radiative transition rate 3.4×10^3 s^{-1} and a very low quantum yield of 4.5×10^{-4}.[15] In the case of O_2 trapped in inert gas matrices, the emission occurs with 0-0 transitions between 1908 and 1924.5 nm with lower transition rates (22 to 105 s^{-1}) and quantum yields close to unity.[13] The measured intensities of the $b\rightarrow a$ and $a\rightarrow X$ emissions are almost equal in this case. The ratio between the radiative transition rates of these two transitions is only weakly matrix-dependent.[13] It can be therefore expected that the $b\rightarrow a$ transition should be observable under 765 nm excitation in SiO_2 as well. However, this conjecture could not be tested in this work because an appropriate detector was not available.

C. Search for the emission from the $b\ ^1\Sigma_g^+$ excited state of O_2 in silica

Luminescence bands caused by a radiative $b\rightarrow X$ transition in O_2 have been reported for O_2 dissolved in CCl_4 (Refs. 14 and 15) and trapped in inert gas crystals.[13] In the former case, the quantum yield is very low ($Q=5\times10^{-8}$) and the observed decay time, $\tau=130$ ns is correspondingly short. In the latter case, the quantum yield of the $b\rightarrow X$ emission is 0.003 to 0.006 with the observed decay times between 9.5 and 46 ms.

A time-resolved luminescence registration technique was used in the previous work[13] to suppress the scattered excitation light and to enable the measurement of the resonance zero-phonon line (ZPL or 0-0 transition). This option was not available in our case. Instead, the very high suppression ($\approx10^{-13}$) of the scattered excitation light by a triple Raman spectrograph was utilized in an attempt to measure either the phonon sidebands of the $b\rightarrow X$ emission while exciting in the

ZPL, or to measure the ZPL in the $b \rightarrow X$ emission spectrum while exciting in the absorption spectrum phonon sidebands.

Measurements of this kind were performed by exciting in the maximum or the high-energy wing of the excitation spectrum of Fig. 3 and recording the Stokes-shifted emission as close as possible to the excitation line. However, in all cases the resulting spectrum was dominated by the conventional Raman spectrum of silica (Fig. 5). This outcome indicates that the quantum yield of the $b \rightarrow X$ transition of O_2 in silica most likely is very low even at $T = 10$ K. The simultaneously observed intense $a \rightarrow X$ emission (Fig. 2) then shows that a radiative or non-radiative $b \rightarrow a$ transition is an important, if not the main, depopulation path of the b state.

The lack of the $b \rightarrow X$ emission together with the observation of long-lived $a \rightarrow X$ emission under the $X \rightarrow b$ excitation (see the Results section) may indicate that it is indeed the a and not the b excited state which has the long lifetime and is the main cause of the slowly decaying $a \rightarrow X$ emission under $X \rightarrow b$ excitation. This is consistent with the conjecture about the relatively high quantum yield of the $a \rightarrow X$ luminescence.

An additional point which could contribute to nonobservation of the $b \rightarrow X$ emission in the current experiments (Fig. 5) would be the possibility of the phonon sidebands in the $X \rightarrow b$ absorption or $b \rightarrow X$ emission being very weak as compared with the ZPL. In inert gas matrices the phonon sidebands and the ZPL's are of comparable intensity, for both the $b \rightarrow X$ and $a \rightarrow X$ transitions.[13] In contrast, for the $a \rightarrow X$ transition of O_2 in silica the amplitude of the phonon sideband is less than 1% from the ZPL intensity (Fig. 2). If this situation can be extrapolated to the $b \rightarrow X$ transition, the intensity of nonresonance luminescence will be very low. Decay time and time-resolved spectral measurements of the resonance ZPL are necessary to clarify this point.

D. The radiation-induced creation of O_2 in glassy silica

The efficient excitation of the $a \rightarrow X$ emission under $X \rightarrow b$ excitation at 765 nm provides a high-sensitivity tool to detect interstitial O_2 in SiO_2. The absolute O_2 concentration in sample 1, Suprasil W1 fused silica was evaluated in our previous Raman work[10] to be 8×10^{17} cm^{-3}. The concentration of O_2 in the other fused silica samples can now be calculated by comparing the relative intensities of the 765 nm excited $a \rightarrow X$ luminescence. The results are shown in Table I. The intensity of the weakest emission band measured (sample 10) corresponds to 2.1×10^{14} O_2/cm^3. As is evident from the Fig. 6, the detection limit of the present measurements is around 5×10^{13} O_2/cm^3.

It is now possible to verify a number of previous conclusions on the creation processes and role of the interstitial O_2 in the radiation processes in SiO_2,[1–7] which were based on the observation of reaction (1) by EPR. The most obvious result is the confirmation of the hypothesis about the radiation-induced creation of interstitial O_2 in silica. As seen from Fig. 6, the O_2 PL band is found in every irradiated glass sample; the only three samples which exhibited no measurable O_2 PL intensity are the nonirradiated ones.

However, this observation still bears an element of uncertainty as regards the ''wet'' silicas [Fig. 6(a)], since correct unirradiated control samples cut from the same glass block were not available for samples 2 to 5. While considered highly improbable in wet silicas, an accidental presence of built-in interstitial O_2 in pristine samples cannot be completely ruled out.

In the case of the oxygen-deficient silicas [Fig. 6(b)], correct unirradiated control samples were available, and it is evident that both neutron and γ-irradiation produce interstitial O_2 molecules in concentrations above 10^{14} cm^{-3}. Since the amounts of the radiation-induced O_2 in oxygen-deficient low-OH fused silica and in the high-OH ''wet'' silica are comparable (Table I), it may be concluded that the destruction of O-H groups is not the main source of oxygen atoms, and that bridging oxygen atoms are involved. A similar conclusion based on EPR data on oxygen-deficient silica and Eq. (1) was drawn recently by Zhang *et al.*[7] The only difference is that they infer an order of magnitude higher concentrations of O_2 (1.5×10^{15} cm^{-3}) after a smaller irradiation dose (0.4 Grad).

There may be several explanations to this discrepancy. Most likely it shows that apart from the diffusion of molecular oxygen [Eq. (1)] there are additional mechanisms leading to creation of POR's on annealing, e.g., reaction of nonbridging oxygen hole center (NBOHC) with atomic oxygen:

$$\equiv \text{Si-O}\cdot + \text{O} \rightarrow \equiv \text{Si-O-O}\cdot. \tag{3}$$

This reaction may be supported by the observation of mutually correlated changes of POR and NBOHC concentrations during annealing and reirradiation cycles.[7] If the fraction of POR's created via reaction (3) is not negligible, the estimates of O_2 concentration based on reaction (1) may be too high.

Other possible causes to the divergent estimates of the radiolytic O_2 concentrations may be different extents of oxygen deficiency in the samples and/or a different character and dose rates of the irradiation (45 kV x rays in Ref. 7 vs γ rays from nuclear reactor irradiation facility in our work).

In all cases the concentration of radiation-induced interstitial O_2 falls far below the concentration of preexisting O_2 in pristine Suprasil W1 silica, 8×10^{17} cm^{-3} (Table I, sample 1). The previous work[8] has shown that the number of interstitial O_2 is actually *reduced* by neutron irradiation in this type of fused silica, more than 10 times for the dose of 10^{19} n/cm^2. Compared with Table I, this corresponds to a concentration below 10^{17} cm^{-3}. Moreover, in wet silica which is initially free of O_2, no measurable quantity of O_2 was found even after a neutron dose of 10^{20} cm^{-2}, corresponding to the creation of less than 5×10^{16} O_2/cm^3, the detection threshold in Ref. 8.[20] This may indicate that some equilibrium concentration of interstitial O_2 in fused silica exists between approximately 10^{16} and 10^{17} O_2/cm^3 for room temperature irradiation, where the creation of new oxygen molecules is balanced by their destruction through direct radio or photolysis or trapping at the active defect sites. There is preliminary evidence[21] based on the defect annealing studies according to reaction (1) that the equilibrium concentration may depend on the dose rate: higher O_2 concentrations are attained under lower γ-irradiation intensities.

One of the fundamental questions in the radiation physics of glassy SiO_2 is whether oxygens can be expelled from their sites in the glass network by relatively low-energy excitonic processes. The data of the present work give no direct an-

swer because of the high-energy irradiations used. Both γ-ray created Compton electrons with energies above 200 keV and neutrons can displace network oxygens by direct knock-on processes. Using the EPR techniques and reaction (1) for the detection, creation of O_2 has been reported during relatively soft irradiations: by 50 kV x-ray irradiation[7] or, most clearly, by two-photon absorption of the 6.4 eV photons from ArF laser.[6] Both these studies rely, however, on the premise that dry oxygen deficient[7] or wet[6] silicas contain negligible amounts of O_2 prior to irradiation. This assumption can not be verified by EPR since no E' centers, which serve as the detectors of O_2, are present in nonirradiated samples. However, it is corroborated by the present work: the concentration of O_2 is below 5×10^{13} in unirradiated wet (sample 6) or dry oxygen deficient (samples 8 and 11) silica. This further strengthens the reported EPR-based evidence[6,7] on the excitonic creation of O_2 in SiO_2.

E. Creation of O_2 in α-quartz

Neutron irradiation of α-quartz monocrystals gives rise to a 765 nm-excited PL band (Fig. 7) which is similar but not completely identical to the PL band of interstitial O_2 observed in glass. It is shifted by 30 to 50 cm^{-1} towards lower energies, and the halfwidth increases from 80 cm^{-1} in glass to $\approx$120 cm^{-1} in crystal. The close values of the transition energies and halfwidths allow this band to be attributed to interstitial O_2 trapped in α-quartz. The O_2 molecules in quartz are most likely created by irradiation, they are present in measurable concentrations only in the heavily neutron-irradiated crystals (samples 12–14).

The differences between the emission spectra in glass and crystal evidently indicate different environments of O_2 in both matrices. The increased halfwidth of the emission peak in quartz may point to a presence of two overlapping subbands; this is most clearly seen for the crystal irradiated by 2.2×10^{18} n/cm^2 (sample 12), indicating that O_2 in quartz is trapped in at least two distinct interstitial sites.

The red-shift of the O_2 emission band from the free-molecule value [7882 cm^{-1} (Ref. 19)] reflects the strength of the O_2-matrix interactions. The peak shifts of O_2 in different solvents were recently systematically studied,[22] and it was concluded that they can be attributed to London dispersion interactions between O_2 and the solvent molecules. The energy of this interaction is proportional to α_{el}/r^6, where α_{el} is the electronic polarizability of the molecules of the interacting medium, and r is the distance between the O_2 and medium particles. Figure 8 shows the dependence of the peak shifts on the refraction index of the medium; the data on organic solvents from Ref. 22 are replotted together with current data on SiO_2. The trend observed in solvents, i.e., that a medium of higher refractive index gives rise to larger peak shifts, holds true also in the cases of glassy and crystalline SiO_2.

However, the data points for SiO_2 in Fig. 8 fall well outside the general tendency. Given the $1/r^6$ dependence of the interaction energy on the (intermolecular) distance, the most probable explanation is that the first coordination sphere of O_2 in solvents, silica and quartz is markedly different. The average size of interstitial sites is larger in silica as compared to α-quartz: while the sizes of the basic structural element,

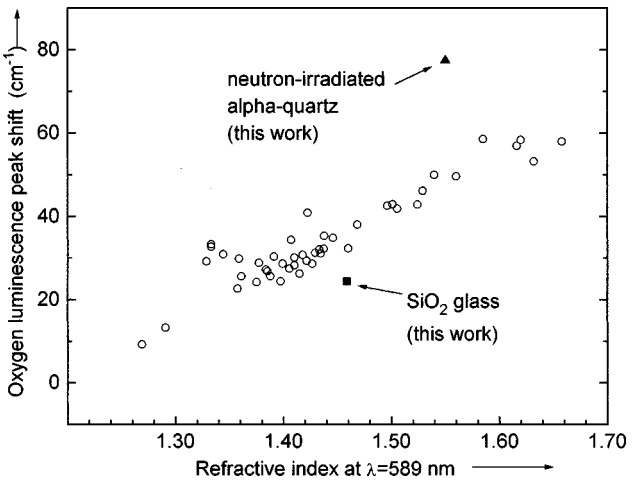

FIG. 8. Peak shifts from the free-molecule value (7882.4 cm^{-1}) of the $a^1\Delta_g \rightarrow X^3\Sigma_g^-$ photoluminescence energy of interstitial oxygen molecules embedded in different media. Circles: different organic solvents, data from Ref. 22; square: Suprasil W1 fused silica; triangle: α-quartz crystal.

the SiO_4 tetrahedron, are almost identical in both forms, the density is much lower in silica (2.20 vs 2.65 g/cm^3). The electronic polarizability of the SiO_2 ''molecule'' can be approximately calculated from the refractive index n and density ρ using the Lorentz-Lorenz equation as

$$\alpha_{el}=\frac{3}{4\pi}\left(\frac{n^2-1}{n^2+2}\right)\frac{m}{\rho}, \tag{4}$$

where m is the mass of the SiO_2 molecule. Using the values of $n=1.46$ for the glass and $n\approx1.55$ for the crystal, α can be calculated to be 2.96×10^{-24} cm^3 and 2.86×10^{-24} cm^3, respectively. Given the similar character of the bonding in silica and α-quartz (corner-sharing SiO_4 tetrahedra), the close values of the electronic polarizabilities are not surprising; the difference in the refractive indices is caused mainly by the different densities of both materials. The much larger peak shift of O_2 luminescence in quartz as compared with silica (Fig. 8) then is directly attributable to a tighter confinement of O_2 in quartz. The calculation of O_2 diffusion in α-quartz[23] has shown that oxygen molecules are heavily compressed even in the relatively large c-axis channels of the α-quartz lattice.

Since the forbidden $a\rightarrow X$ emission transition and (to a lesser degree[13]) $X\rightarrow b$ excitation transition of O_2 are strongly enhanced by the O_2-matrix interactions, the different environments of O_2 in quartz and silica in general mean different PL quantum yields and excitation cross sections. This may introduce an uncertainty when calculating the absolute concentration of O_2 in quartz by simple scaling of the PL intensity relative to the standard silica sample with a known concentration of O_2 (sample 1 in Table I). The general trend, reported for O_2 in solvents, is that larger PL peak shifts are associated with larger $a\rightarrow X$ radiative transition rates (k_r).[22] For the differences in peak shifts of 40 cm^{-1}, an up to ten fold increase of k_r is reported. Difference between the PL peak positions in α-quartz and silica is of similar size, and by analogy, a similar relation between k_r values in both materials may exist. If the nonradiative rate k_{nr} [Eq. (2)] is not

negligible, an increase of the quantum yield and of the PL intensity for O_2 in α-quartz may take place. The values of O_2 concentration in quartz crystals (Table I) then most likely define the upper concentration limits. However, in the light of the evidence for a relatively high quantum yield in the case of O_2 in glass (Sec. IV A), its increase in quartz may actually be small.

There is no detectable luminescence of O_2 in α-quartz crystal after the γ-irradiation dose of 2.2 Grad while O_2 is found in each of the similarly irradiated glass samples (2, 4, and 10). This finding may indicate that the glassy state assists the creation of O_2 in some way, e.g., by providing trapping sites for the radiation-induced mobile interstitial oxygen atoms and thus impeding their recombination with oxygen vacancies.

V. CONCLUSION

This study has demonstrated sensitive photoluminescence techniques to monitor the interstitial O_2 molecules in SiO_2. The creation of radiolytic O_2 in fused silica in concentrations between 10^{14} and 10^{16} O_2/cm^3 is confirmed by direct measurements. Evidence on the creation of radiation-induced O_2 in α-quartz crystals is obtained. Similar techniques are evidently applicable as well to other solid state materials with interstitial sites large enough to accommodate O_2 molecules without a significant charge transfer taking place.

The interstitial O_2 is an aggregate defect itself, and as such it is just one of the numerous possible intrinsic defects in SiO_2. However, it is the most direct successor to an elementary radiation defect in oxides, an interstitial O atom. While the other member of the elementary Frenkel pair, the oxygen vacancy is extensively studied in many oxide materials, including SiO_2,[1] the interstitial oxygen still remains elusive. It may be hoped that the added ability to monitor the creation and destruction of O_2 will provide additional means of verifying the models concerning the expulsion of oxygen atoms from the lattice sites in exciton self-trapping processes in SiO_2 and their part in the successive defect processes.

ACKNOWLEDGMENTS

The authors are grateful to R. Kröhnert and H. Niemann for help with setting up some experiments. This work was partially supported by Latvian Science Council Grant No. 960658.

[1] D. L. Griscom, J. Ceram. Soc. Jpn. **99**, 923 (1991).
[2] R. L. Pfeffer, in *The Physics and Technology of Amorphous* SiO_2, edited by R. A. B. Devine (Plenum, New York, 1988), p. 181.
[3] M. Stapelbroek, D. L. Griscom, E. J. Friebele, and G. H. Sigel, Jr., J. Non-Cryst. Solids **32**, 313 (1979).
[4] A. H. Edwards and W. Beall-Fowler, Phys. Rev. B **26**, 6649 (1982).
[5] L. Zhang, V. A. Mashkov, and R. G. Leisure, Phys. Rev. Lett. **74**, 1605 (1995).
[6] T. E. Tsai and D. L. Griscom, Phys. Rev. Lett. **67**, 2517 (1991).
[7] L. Zhang, V. A. Mashkov, and R. G. Leisure, Phys. Rev. B **53**, 7182 (1996).
[8] L. Skuja and B. Güttler, Phys. Rev. Lett. **77**, 2093 (1996).
[9] W. Carvalho, P. Dumas, J. Corset, and V. Neuman, J. Raman Spectrosc. **16**, 330 (1985).
[10] L. Skuja, B. Güttler, D. Schiel, and A. Silin, J. Appl. Phys. **83**, 6106 (1998).
[11] B. Minaev, O. Vahtras, and H. Agren, Chem. Phys. **208**, 299 (1996).
[12] H. Hosono, H. Kawazoe, and N. Matsunami, Phys. Rev. Lett. **80**, 317 (1998).
[13] G. Tyczkowski, U. Schurath, M. Bodenbinder, and H. Willner, Chem. Phys. **215**, 379 (1997).
[14] R. Schmidt and M. Bodesheim, J. Phys. Chem. **98**, 2874 (1994).
[15] R. Schmidt and M. Bodesheim, J. Phys. Chem. **99**, 15 919 (1995).
[16] F. L. Galeener, A. J. Leadbetter, and M. W. Stringfellow, Phys. Rev. B **27**, 1052 (1983).
[17] W. Heitmann, H. U. Bonewitz, and A. Mühlich, Electron. Lett. **19**, 616 (1983).
[18] O. Humbach, H. Fabian, U. Grzesik, U. Haken, and W. Heitmann, J. Non-Cryst. Solids **203**, 19 (1996).
[19] P. H. Krupenie, J. Phys. Chem. Ref. Data **1**, 423 (1972).
[20] The type-III ''wet'' sample irradiated by 10^{20} n/cm^2 was not available during the present series; therefore an exact concentration of O_2 could not be measured for this neutron fluence. Most likely it is 10^{15}–10^{16} cm^{-3} (compare to data on type-III silicas in Table I).
[21] D. L. Griscom (private communication).
[22] J. M. Wessels and M. A. Rodgers, J. Phys. Chem. **99**, 17 586 (1995).
[23] M. I. Heggie, R. Jones, C. D. Latham, S. C. P. Maynard, and P. Tole, Philos. Mag. B **65**, 463 (1992).